Am J Physiol Lung Cell Mol Physiol 313: L406–L415, 2017.
First published May 4, 2017; doi:10.1152/ajplung.00107.2017.

RESEARCH ARTICLE

$GABA_A$ receptor α_4-subunit knockout enhances lung inflammation and airway reactivity in a murine asthma model

Gene T. Yocum,[1] Damian L. Turner,[2] Jennifer Danielsson,[1] Matthew B. Barajas,[1] Yi Zhang,[1] Dingbang Xu,[1] Neil L. Harrison,[1,3] Gregg E. Homanics,[4] Donna L. Farber,[2,5] and Charles W. Emala[1]

[1]*Department of Anesthesiology, Columbia University, New York, New York;* [2]*Columbia Center for Translational Immunology, New York, New York;* [3]*Department of Pharmacology, Columbia University, New York, New York;* [4]*Departments of Anesthesiology, Neurobiology, and Pharmacology and Chemical Biology, University of Pittsburgh, Pittsburgh, Pennsylvania; and* [5]*Department of Surgery and Microbiology and Immunology, Columbia University, New York, New York*

Submitted 7 March 2017; accepted in final form 30 April 2017

Yocum GT, Turner DL, Danielsson J, Barajas MB, Zhang Y, Xu D, Harrison NL, Homanics GE, Farber DL, Emala CW. $GABA_A$ receptor α_4-subunit knockout enhances lung inflammation and airway reactivity in a murine asthma model. *Am J Physiol Lung Cell Mol Physiol* 313: L406–L415, 2017. First published May 4, 2017; doi:10.1152/ajplung.00107.2017.—Emerging evidence indicates that hypnotic anesthetics affect immune function. Many anesthetics potentiate γ-aminobutyric acid A receptor ($GABA_AR$) activation, and these receptors are expressed on multiple subtypes of immune cells, providing a potential mechanistic link. Like immune cells, airway smooth muscle (ASM) cells also express $GABA_ARs$, particularly isoforms containing α_4-subunits, and activation of these receptors leads to ASM relaxation. We sought to determine if $GABA_AR$ signaling modulates the ASM contractile and inflammatory phenotype of a murine allergic asthma model utilizing $GABA_AR$ α_4-subunit global knockout (KO; *Gabra4*$^{o/o}$) mice. Wild-type (WT) and *Gabra4* KO mice were sensitized with house dust mite (HDM) antigen or exposed to PBS intranasally 5 days/wk for 3 wk. Ex vivo tracheal rings from HDM-sensitized WT and *Gabra4* KO mice exhibited similar magnitudes of acetylcholine-induced contractile force and isoproterenol-induced relaxation (P = not significant; n = 4). In contrast, in vivo airway resistance (flexiVent) was significantly increased in *Gabra4* KO mice ($P < 0.05$, $n = 8$). Moreover, the *Gabra4* KO mice demonstrated increased eosinophilic lung infiltration ($P < 0.05$; $n = 4$) and increased markers of lung T-cell activation/memory (CD62L low, CD44 high; $P < 0.01$, $n = 4$). In vitro, *Gabra4* KO $CD4^+$ cells produced increased cytokines and exhibited increased proliferation after stimulation of the T-cell receptor as compared with WT $CD4^+$ cells. These data suggest that the $GABA_AR$ α_4-subunit plays a role in immune cell function during allergic lung sensitization. Thus $GABA_AR$ α_4-subunit-specific agonists have the therapeutic potential to treat asthma via two mechanisms: direct ASM relaxation and inhibition of airway inflammation.

house dust mite antigen; lymphocyte; eosinophil; flexiVent; organ bath

A RECEPTOR-OPERATED chloride channel, the γ-aminobutyric acid A receptor ($GABA_AR$) is well known for its role in inhibitory neurotransmission in the central nervous system (CNS). We have previously demonstrated that airway smooth muscle (ASM) cells express $GABA_ARs$ and that activation of these receptors leads directly to ASM relaxation (8, 26). $GABA_ARs$ are heteropentamers that generally contain two α-subunits (α_{1-6}), two β-subunits (β_{1-3}), and a fifth subunit that can be γ (γ_{1-3}), δ, ε, θ, or π. Among the six α-subunit subtypes, human ASM cells express only α_4 and α_5 (9), providing the opportunity for α-subunit-selective pharmacologic targeting to alleviate bronchoconstriction while avoiding the sedation largely mediated by α_{1-3}-containing receptors in the CNS (10, 45).

Several immune cells also express functional $GABA_ARs$, including monocytes, macrophages, mast cells, and lymphocytes, and modulation of these receptors has been shown to affect cell function in vitro (1, 3, 7, 13, 25, 32, 36, 43). Clinical trials have also suggested that pharmacologic activation of $GABA_ARs$ may be immunomodulatory. For example, studies demonstrated that critically ill patients sedated with benzodiazepines, positive $GABA_AR$ modulators, suffered increased infections (33) and increased mortality from sepsis (28) compared with patients sedated with a drug that works via $GABA_AR$-independent mechanisms. Furthermore, a subsequent animal study demonstrated that subsedative doses of a benzodiazepine increased mortality in a murine pneumonia model, presumably due to immune suppression (34).

Chronic airway inflammation and ASM hyperresponsiveness are both hallmarks of asthma, a disease that affects hundreds of millions worldwide (24). Asthma is frequently studied in mice using house dust mite (HDM) antigen sensitization, a model that mimics the predominant subtype of human allergic/inflammatory asthma dominated by Th2-mediated inflammation. Given the potential role that $GABA_AR$ activation plays in immune modulation, we hypothesized that global genetic deletion of the $GABA_AR$ α_4-subunit (*Gabra4*) would lead to increased airway reactivity and inflammation in HDM-sensitized mice.

MATERIALS AND METHODS

Mice. All studies were approved by the Columbia University Institutional Animal Care and Use Committee. Eight- to ten-week-old male mice with a global genetic deletion of the $GABA_AR$ α_4-subunit (*Gabra4*$^{o/o}$; *Gabra4* KO) (5), and their corresponding background wild-type C57BL/6J mice (WT) were utilized.

RT-PCR survey of $GABA_AR$ subunit expression. Mouse spleens were harvested, minced, and passed through a 40-μM cell strainer to obtain dispersed splenocytes. After red blood cell lysis, $CD4^+$ cells were isolated by negative selection using a magnetic separation kit

Address for reprint requests and other correspondence: G. T. Yocum, Dept. of Anesthesiology, Columbia Univ., 622 W. 168th St., P&S Box 46, New York, NY 10032 (e-mail: gty2102@cumc.columbia.edu).

(MagniSort Mouse CD4$^+$ T Cell Enrichment Kit; eBioscience, San Diego, CA). Total RNA was obtained from these CD4$^+$ lymphocytes and D10 cells (murine Th2 cell line; gift of Dr. X. M. Li, Mt. Sinai Hospital, New York, NY) using Trizol Reagent, and cDNA was synthesized using SuperScript VILO reagents (Thermo Fisher Scientific, Waltham, MA). Two micrograms of RNA were used for each 20-μl RT-PCR reaction. PCR was then performed (40 cycles) using 1 μl of cDNA product as the templates and primers specific for each $GABA_AR$ subunit (primer sequences are listed in Table 1; Advantage 2 Polymerase Mix; Clontech, Mountain View, CA). All primer sets were designed to flank exon splice sites to avoid confounding replication of genomic DNA (genomic DNA replicates would be significantly larger). Two-step PCR was used with a denaturing temperature of 94°C for 10 s and an annealing/amplification temperature of 68°C for 1 min (30 cycles). Mouse whole brain served as a positive control, and PCR reaction mixtures devoid of cDNA served as RT-PCR negative controls (all reagents were from Life Technologies, Carlsbad, CA).

HDM antigen sensitization. While spontaneously breathing under brief (2 to 3 min) isoflurane (Baxter, Deerfield, IL) anesthesia, both WT and *Gabra4* KO mice were exposed to intranasal purified HDM antigen (30 μg; Greer, Lenoir, NC) dissolved in 25 μl PBS or PBS alone (nonsensitized control) once daily (Monday-Friday) for 3 wk.

In vivo airway resistance and lung compliance testing. In vivo airway resistances were assessed using a flexiVent FX1 module with an inline nebulizer (SciReq, Montreal, QC, Canada), as previously described (37, 38), using HDM-sensitized and nonsensitized (PBS controls) WT and *Gabra4* KO mice. Briefly, the mice were anesthetized with intraperitoneal pentobarbital (50 mg/kg), paralyzed with intraperitoneal succinylcholine (10 mg/kg), and mechanically ventilated via a tracheostomy (tidal volume: 10 mg/kg, 150 breaths/min). Airway resistances were measured during a graded, nebulized methacholine challenge. Each nebulization period was 10 s with a 50% duty cycle using a 4- to 6-μm nebulizer. EKG and temperature monitoring was performed throughout the experiment. Central airway resistance values (Rn) and lung compliance (Crs) for each mouse at

Table 1. *Primer sequences utilized for RT-PCR analyses of $GABA_AR$ subunit mRNA expression in murine cells*

$GABA_AR$ Subunit (Accession No.)	Primer Sequence 5′ to 3′	Product Size, bp
α_1 (NM_010250)		
Forward	CTA TGG ACA GCC CTC CCA AGA TGA ACT TA	147
Reverse	GTG ACG AAA ATG TCG GTC TTC ACT TCA GTT A	
α_2 (NM_008066)		
Forward	GAA CAG AGA ATC GGT GCC AGC AAG A	175
Reverse	TGC AAA TTC AAT TAG GGC AGA GAA CAC AA	
α_3 (NM_008067)		
Forward	GGT TCA TAG CCG TCT GTT ATG CCT TTG TA	158
Reverse	GTT TTT CTT TGT TGG AGC TGC TGG TGT TT	
α_4 (NM_010251)		
Forward	CCT GTG CTG AAG GAG AAA CAC ACA GAA	210
Reverse	GAA TGG ATT TGG ACT GGA AGC TAA GTG A	
α_5 (NM_076942)		
Forward	TGC TAT GCA TTT GTC TTC TCT GCT CTG ATT	182
Reverse	GGA GGA TGG GTC AGC TTT CCA GTT GTA A	
α_6 (NM_076942)		
Forward	GTC TGA ATC CCT GCA AGC AGA GAT TGT T	138
Reverse	TTT AAG ATG GGC GTT CTA CTG AGG GCT TT	
β_1 (NM_008069)		
Forward	GTC TGA ATC CCT GCA AGC AGA GAT TGT T	138
Reverse	TTT AAG ATG GGC GTT CTA CTG AGG GCT TT	
β_2 (NM_008070)		
Forward	GGG TGC CTG ACA CCT ACT TCC TGA ATG ATA	175
Reverse	CAG TTT TGT TCA TCC AGT GGA TAC CGC CTT	
β_3 (NM_008071)		
Forward	GAC CTC AGA AGA TAC CCA CTG GAT GAG CAA	169
Reverse	AGA CCA GAC GGT GCT CTA CAA TGG AGA A	
γ_1 (NM_010252)		
Forward	GGA ATA CGG AAC CTT GCA TTA TTT TAC TAG CAA CA	175
Reverse	CAA ACA CTG GTA GCC ATA ATC ATC TTC CCC TT	
γ_2 (NM_008073)		
Forward	GAC GCT GTG GAT TCT GCT CCT GCT AT	121
Reverse	CTC TGG AAC TTT TGG AGT CAA CAC CCA T	
γ_3 (NM_008074)		
Forward	GCC AGC TGC AAC TGC ATA ACT TCC CT	156
Reverse	AGT CAA ACT GAT AGA GCC GCC ATG AT	
δ (NM_008072)		
Forward	CCA GTT CAC TAT CAC CAG TTA CCG CTT CAC	441
Reverse	GCG TTC CTC ACA TCC ATC TCT GCC CTT	
ε (NM_017369)		
Forward	CAC ATG CTC AAT TTT CCA ATG GAT TCT CAC TCT T	377
Reverse	AGC GTG GCC ATG GTG AGC ACA GAA CTG AC	
θ (NM_020488)		
Forward	CTG TTC CCT GGA TCT GCA AAA ATT CCC TAT GGA C	346
Reverse	TAC CCT GGC TGC AGA GGA ATC ATA GTT CAT CCA A	
π (NM_146017)		
Forward	GAG AAC CTG CAT TGG AGT GAC AAC GGT GTT A	320
Reverse	AGT TGA CAT TGT CAC CAG AGA TTT CAA TGC T	

$GABA_AR$, γ-aminobutyric acid A receptor.

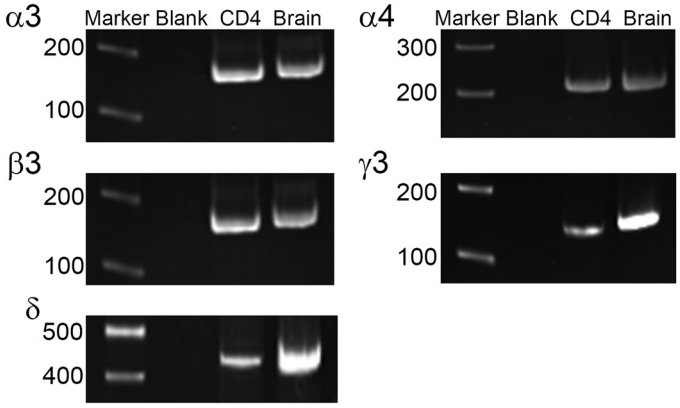

Fig. 1. Gel electrophoresis images from RT-PCR survey of γ-aminobutyric acid A receptor ($GABA_AR$) subunit expression in mouse primary $CD4^+$ lymphocytes. mRNA was detected for multiple $GABA_AR$ subunits, including α_4 and all other subunits needed to form a functional channel. The full results are summarized in Table 2. Marker: basepair length marker; Blank: PCR reaction devoid of cDNA (negative control); CD4: murine $CD4^+$ lymphocyte; Brain: murine brain (positive control).

each methacholine dose represent an average of three forced oscillatory measurements. Data were compared between groups by assessing the area under the methacholine cumulative dose-response curve.

Ex vivo tracheal ring organ bath experiments. Tracheal ring organ bath experiments were conducted as described previously (37). Briefly, tracheas were rapidly removed from 3-wk HDM-sensitized and nonsensitized WT and *Gabra4* KO mice and placed in modified Krebs-Henseleit buffer of the following composition (in mM): 115 NaCl, 2.5 KCl, 1.91 $CaCl_2$, 2.46 $MgSO_4$, 1.38 NaH_2PO_4, 25 $NaHCO_3$, and 5.56 D-glucose at pH 7.4. The tracheas were then mounted in a myograph (DMT, Ann Arbor, MI) and held at a resting tension of 5 mN for 1 h at 37°C in buffer continuously bubbled with 95% O_2-5% CO_2 (buffer was exchanged every 15 min). Following this equilibration period, three acetylcholine (ACh) dose-response curves were constructed (ACh at 100 nM to 1 mM) with extensive buffer exchanges and a resetting of resting tension to 5 mN between dose-response challenges. An ACh EC_{50} was determined for each tracheal ring. The maximum ACh-induced contractile force generated was compared between groups.

To compare relaxation in response to the β-agonist isoproterenol between groups, tracheal rings were contracted with an EC_{50} ACh concentration and contractile force were allowed to plateau. Increasing concentrations of isoproterenol (0.1 nM to 10 μM in half-log increments) were then added at 7-min intervals as contraction force was continuously measured.

Lung histology. Whole lungs were obtained from HDM-sensitized WT and *Gabra4* KO immediately following pentobarbital overdose and fixed with 10% formalin overnight. The lungs were subsequently dehydrated through a graded ethanol series, paraffin embedded, sectioned, dewaxed, and stained with hematoxylin and eosin for histologic analysis. Lung inflammation was quantified using the composite lung inflammation index (16).

Lung immune cells count differentials and flow cytometric studies. Whole lungs were obtained from nonsensitized and HDM-sensitized WT and *Gabra4* KO mice immediately following intraperionteal pentobarbital overdose and PBS perfusion via right heart puncture. To isolate the intrapulmonary inflammatory cells, the lungs were quickly minced and enzymatically digested in 5 ml of 1 mg/ml type IV collagenase (Sigma, St. Louis, MO), 1 mg/ml trypsin inhibitor, and 0.1 mg/ml DNAase I (Thermo Fisher Scientific) in PBS at 37°C for 30 min. The tissues were then gently crushed through a 70-μm strainer, and the cells were collected and washed with PBS.

Smears were prepared for cell differential analysis conducted by an independent pathologist. Cells were also resuspended in FACS buffer at 5×10^5 cells/ml and stained with antibodies (CD4, CD8, CD62L, and CD44; BD Bioscience, San Diego, CA) at 1:200 dilution and room temperature for 30 min (helper T cells: CD4+/CD8−; cytotoxic T cells: CD8+/CD4−; and marker of activation/memory T cells: $CD62L^{LOW}/CD44^{HIGH}$) for flow cytometric analyses using a LSRII Flow Cytometer (BD Biosciences) and FlowJo software (FlowJo, Ashland, OR).

In vitro $CD4^+$ cell activation. $CD4^+$ cells were isolated from WT and *Gabra4* KO mice and loaded with a fluorescein diacetate proliferation dye and placed into culture. The cells were then stimulated with anti-CD3/CD28-coated beads (Dynabeads Mouse T-Activator; Thermo Fisher Scientific) for 96 h. Cell culture supernatants were collected at 16, 24, 48, 72, and 96 h for cytokine concentration analyses using a cytometric bead array kit and a Canto II flow cytometer (Mouse Th1/Th2/Th17 Cytokine Kit; BD Biosciences). Cell proliferation index (divisions/cell) was accessed at 72 h.

Statistical analysis. Where appropriate, two-tailed Student's *t*-tests or one-way ANOVA with Bonferroni posttest comparisons were employed using Prism 4.0 software (GraphPad, San Diego, CA). Data are presented as means ± SE; $P < 0.05$ was considered significant. Numbers refer to number of mice for in vivo experiments and number of mouse tissue donors for ex vivo and in vitro experiments.

RESULTS

Murine $CD4^+$ cells express multiple $GABA_AR$ subunit mRNAs. RT-PCR analysis revealed the presence of mRNA for multiple $GABA_AR$ subunits in mouse Th2 lymphocytes (D10 cells) and freshly isolated mouse $CD4^+$ cells, including the $GABA_AR$ α_4-subunit (Fig. 1 and Table 2). Furthermore, there was expression of all necessary subunits to form functional $GABA_ARs$ (α- and β-subunits and several "tertiary" subunits). All primer sets were designed to flank introns to avoid replication of genomic DNA and produced PCR products of predicted size using positive control cDNA (mouse brain). PCR reactions devoid of cDNA (labeled blank in Fig. 1) served as negative controls.

HDM-sensitized Gabra4 KO mice have increased in vivo airway resistance and decreased lung compliance compared with HDM-sensitized WT mice. HDM antigen sensitization led to a significant increase in in vivo airway resistance during an inhaled methacholine challenge in both WT and *Gabra4* KO

Table 2. *RT-PCR survey of $GABA_AR$ subunit mRNA expression in D10 cells and mouse primary $CD4^+$ lymphocytes*

Subunit	D10	$CD4^+$
α_1	−	−
α_2	−	−
α_3	+	+
α_4	+	+
α_5	−	−
α_6	+	−
β_1	+	−
β_2	+	−
β_3	+	+
γ_1	−	−
γ_2	+	−
γ_3	+	+
δ	−	+
ε	−	−
θ	+	−
π	−	−

+, mRNA detected; −, mRNA not detected.

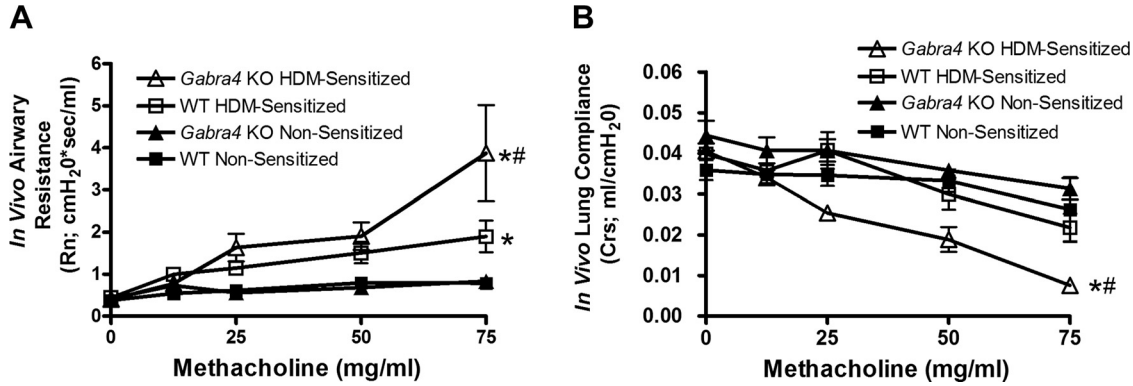

Fig. 2. In vivo mouse airway resistance and lung compliance during a graded inhaled methacholine challenge. *A*: house dust mite (HDM) sensitization led to a significantly increased central airway resistance (Rn) in both wild-type (WT) and *Gabra4* knockout (KO) mice compared with their corresponding nonsensitized controls (*$P < 0.01$). Notably, HDM-sensitized *Gabra4* KO mice were significantly more reactive than HDM-sensitized WT mice (#$P < 0.05$). *B*: HDM-sensitized *Gabra4* KO mice also demonstrated increased lung compliance (Crs) compared with both HDM-sensitized WT mice (#$P < 0.05$) and nonsensitized *Gabra4* KO mice (*$P < 0.01$). Areas under the curves were compared by ANOVA with Bonferroni post hoc comparisons. Data are means ± SE; $n = 8$ mice.

mice (Fig. 2*A*; area under curve compared by ANOVA with Bonferroni post hoc comparison, *$P < 0.01$; $n = 8$ mice) compared with their corresponding nonsensitized (PBS) controls. Notably, HDM-sensitized *Gabra4* KO mice had significantly higher resistance than HDM-sensitized WT mice (#$P < 0.05$; $n = 8$ mice). The effect of methacholine dosage on airway resistance was significant for each group (ANOVA, $P < 0.05$). Furthermore, HDM-sensitized *Gabra4* KO mice had decreased lung compliance compared with both nonsensitized *Gabra4* KO mice (Fig. 2*B*; *$P < 0.01$) and HDM-sensitized WT mice (#$P < 0.05$, area under curve compared by ANOVA with Bonferroni post hoc comparison).

Ex vivo tracheal ring contractile properties do not differ between Gabra4 KO and WT mice. Although sensitized *Gabra4* KO mice had higher in vivo airway resistances than sensitized WT mice, tracheal ring isolated from the two groups showed similar ex vivo contractile responses following ACh exposure, both in dose responses to ACh and maximum ACh-induced contractile force (Fig. 3, *A* and *B*; ANOVA and Student's *t*-test, P = ns; $n = 4$ mice). The tracheal rings from both groups also displayed similar relaxation responses to the β-agonist isoproterenol (Fig. 3*C*; Student's *t*-test, P = ns; $n = 4$ mice), suggesting that the difference seen in in vivo airway reactivity between HDM-sensitized WT and *Gabra4* KO mice is not likely a result of intrinsic differences in ASM reactivity but more likely due to enhanced lung inflammation.

Gabra4 KO mice have heightened eosinophilic lung inflammation following HDM sensitization compared with WT mice. Quantitative analyses of hematoxylin and eosin sections from HDM-sensitized WT and *Gabra4* KO mice demonstrated

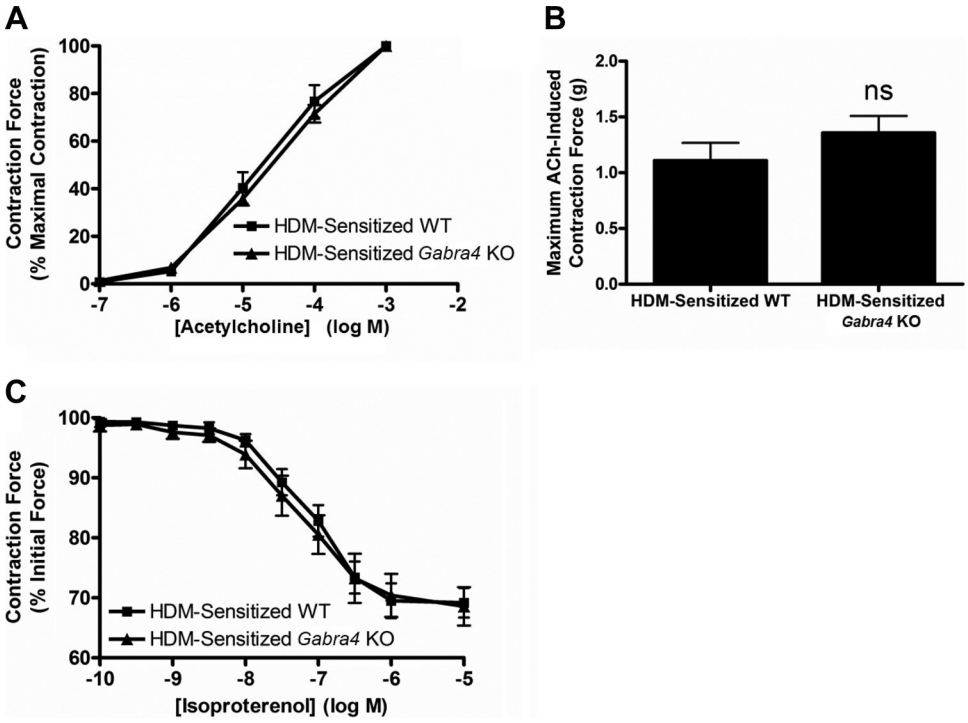

Fig. 3. Ex vivo tracheal ring organ bath experiments with HDM-sensitized mice. *A*: acetylcholine (ACh) dose-response curve for tracheal rings from WT and *Gabra4* KO mice. Contraction forces as a percentage of maximal acetylcholine-induced contraction are not significantly different. *B*: absolute contraction force generate by 1 mM ACh is also not significantly different between groups. *C*: relaxation of an acetylcholine EC_{50} contraction by the β-agonist isoproterenol was not significantly different between tracheal rings from WT and *Gabra4* KO mice. Data are means ± SE; ns, not significant by Student's *t*-test; $n = 4$ mice for all.

greater inflammatory infiltration in the *Gabra4* KO mice (Fig. 4; quantified in Fig. 4*C* using composite lung inflammation score (16); ANOVA with Bonferroni post hoc comparisons, $*P < 0.05$; $n = 4$ mice). This was particularly evident in the perivascular and peribronchial regions (Fig. 4*B*, *inset*). Following enzymatic lung digestion and inflammatory cell collection, differential cell count analyses demonstrated that HDM-sensitized *Gabra4* KO mice had a significantly higher percentage of intrapulmonary eosinophils compared with HDM-sensitized WT mice (Fig. 4*D*; 68.5 ± 13.6 vs. 11.6 ± 6.4%; ANOVA with Bonferroni post hoc comparisons, $P < 0.05$; $n = 4$ mice). Lymphocyte and neutrophil differential counts were not significantly different between groups.

Forward scatter/side scatter (FSC/SSC) flow cytometric analyses showed no significant differences between lung digest cells from nonsensitized WT and *Gabra4* KO mice. However, when HDM-sensitized groups were examined, *Gabra4* KO had an increase in cells with FSC/SSC characteristics consistent with granulocytes (red circle), presumably eosinophils given the results presented in Fig. 4*D*, and a relative loss of lymphocytes (black circles in Fig. 5*A*). However, despite a loss of lymphocytes apparent on the FSC/SSC plot, those CD4+ cells present in *Gabra4* KO express a higher level of cell activation/memory markers ($CD62L^{LOW}/CD44^{HIGH}$) (Fig. 5*A*; quantified in Fig. 4*B*; 64.5 ± 1.7 vs. 44.9 ± 0.4%; Student's *t*-test, $P < 0.01$; $n = 4$ mice) suggesting that at a 3-wk time point the $CD4^+$ cells from *Gabra4* KO mice had undergone sustained activation resulting in their apoptotic depletion.

Gabra4 $CD4^+$ cells demonstrate heightened cellular activation in vitro compared with WT $CD4^+$ cells. Given the key role helper T cells ($CD4^+$ lymphocytes) play in orchestrating allergic lung inflammation (42) and the in vivo suggestion that the $CD4^+$ cells from *Gabra4* KO mice had undergone sustained activation resulting in their depletion, we chose to compare *Gabra4* KO and WT $CD4^+$ cells function in vitro. Following activation of the T-cell receptor with anti-CD3/CD28 coated beads in vitro, *Gabra4* $CD4^+$ cells expressed higher levels of several cytokines compared with WT controls, including several proinflammatory cytokines (IL-2, INF-γ, IL-6, and IL-17A) at several time points (Fig. 6; ANOVA with Bonferroni post hoc test, $*P < 0.05$, $***P < 0.001$; $n = 3$ mice). Consistent with these findings, *Gabra4* $CD4^+$ cells proliferated to a greater extent than WT $CD4^+$ cells after 72 h of stimulation in vitro (Fig. 7, *A* and *B*; Student's *t*-test, $**P <$

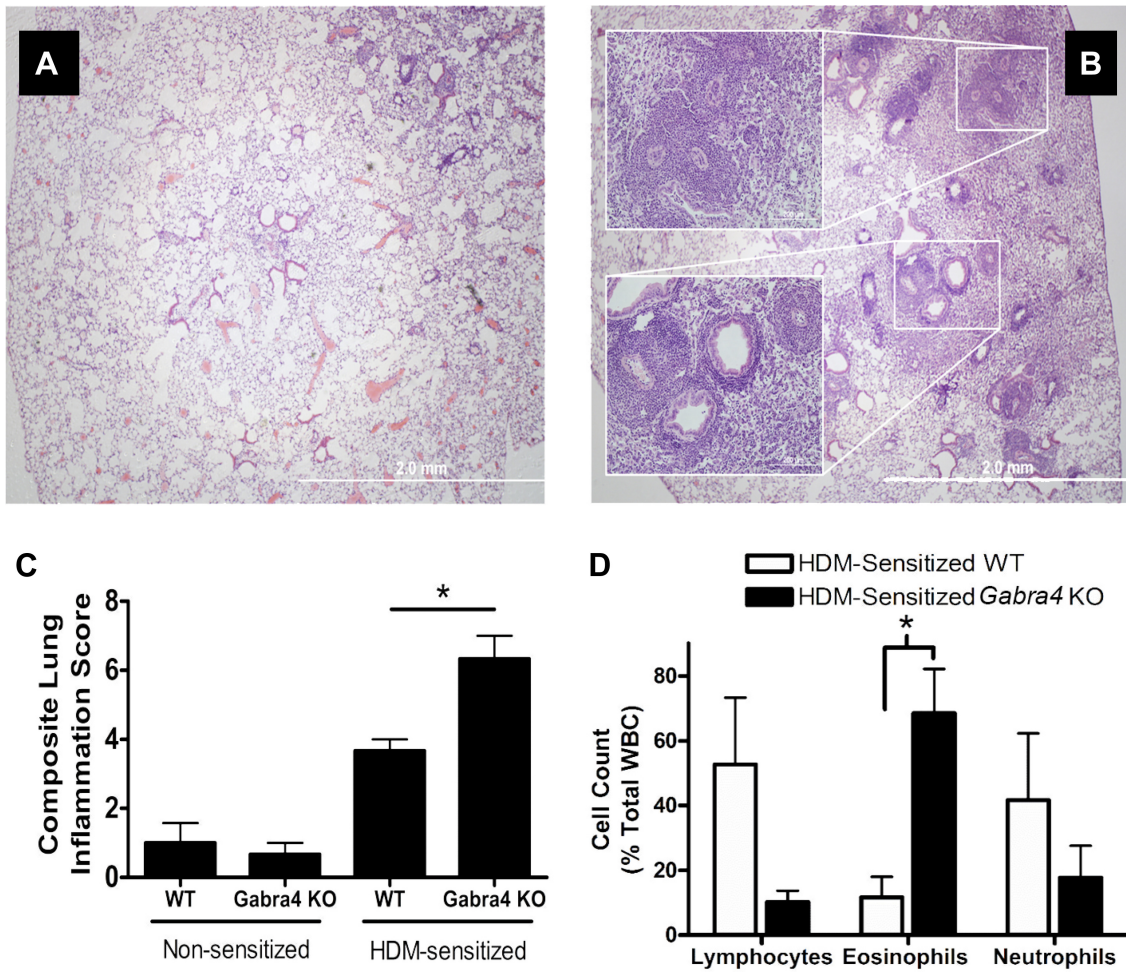

Fig. 4. Hematoxylin and eosin-stained lung sections from HDM-sensitized (*A*) WT and (*B*) *Gabra4* KO mice. KO mice exhibit enhanced perivascular and peribronchial inflammatory infiltration after 3 wk of intranasal HDM sensitization. *C*: lung inflammation was quantified using the lung composite lung inflammation score (16), which demonstrated *Gabra4* KO lungs were significantly more inflamed than WT lungs. *D*: HDM-sensitized *Gabra4* KO mice have a significantly larger proportion of invading eosinophils than HDM-sensitized WT mice. Data are means ± SE; $n = 4$ mice. $*P < 0.05$ by ANOVA with Bonferroni post hoc comparisons.

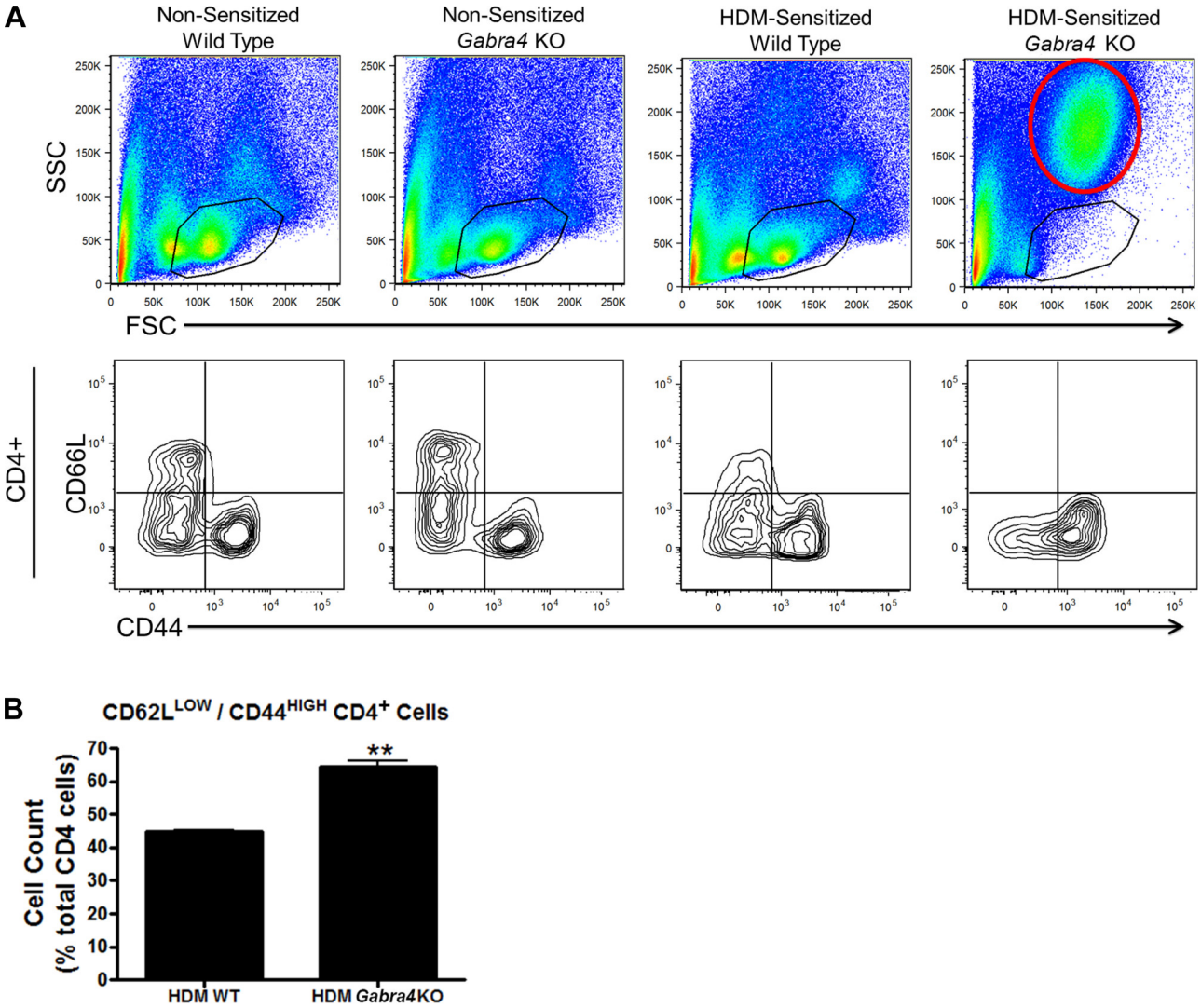

Fig. 5. *A*: representative figures from flow cytometry analyses of mouse lung immune cells. Forward scatter/side scatter (FSC/SSC) plots of lung digests from nonsensitized (PBS) and HDM-sensitized WT and *Gabra4* KO and mice are presented at *top*. The black circles contain cells with FSC (size) and SSC (granularity) values characteristic of lymphocytes. HDM-sensitized *Gabra4* KO mice have a decrease in lymphocytes and an increase in granulocytes (area outline in red at *top right*) based on FSC/SSC analysis. Despite a decreased percentage of lymphocytes in the total lung digest, those $CD4^+$ cells present in HDM-sensitized *Gabra4* KO mice express increased markers of T-cell activation/memory ($CD62L^{LOW}/CD44^{HIGH}$). This is represented in the *bottom right* quadrants in *A* and is quantified in *B*. Data are means ± SE; $n = 4$ mice. $^{**}P < 0.01$ by Student's *t*-test.

0.01; $n = 3$ mice). These in vitro studies suggest an innate difference between *Gabra4* KO and WT lymphocyte cellular function exhibited by enhanced and more sustained activation following stimulation.

DISCUSSION

The results presented here demonstrate that global knockout of the $GABA_AR$ α_4-subunit leads to a greater degree of lung inflammation and in vivo airway reactivity in a murine model of inflammation/allergic asthma. Despite this increase in in vivo resistance, ex vivo tracheal ring organ bath experiments demonstrate that the ASM from these mice behaves similarly when removed from the in vivo inflammatory milieu, both in terms of contraction in response to a muscarinic agonist and relaxation in response to a β-agonist. Therefore, the in vivo airway reactivity difference demonstrated between WT and $GABA_AR$ α_4-subunit KO mice is not likely due to a primary ASM effect, despite the fact ASM expresses $GABA_ARs$ containing α_4-subunits (9, 45).

Histologic analysis demonstrates a striking increase in inflammatory cell infiltration in sensitized *Gabra4* KO mice, particularly eosinophils, which are key mediators of the Th2-predominant subtype of asthma (4, 41). Notably, flow cytometric analyses revealed a loss of the lung lymphocyte population in HDM-sensitized *Gabra4* KO mice, even though the remaining $CD4^+$ cells expressed higher levels of markers of T-cell activation/memory. Given the heightened level of eosinophilic infiltration presumably orchestrated by activated $CD4^+$ T cells and resident innate immune cells, this suggests that these lymphocytes may have become apoptotic during the prolonged 3-wk period of allergic sensitization. Regardless, this enhanced inflammation is likely the cause of the heightened in vivo airway reactivity demonstrated in *Gabra4* KO mice.

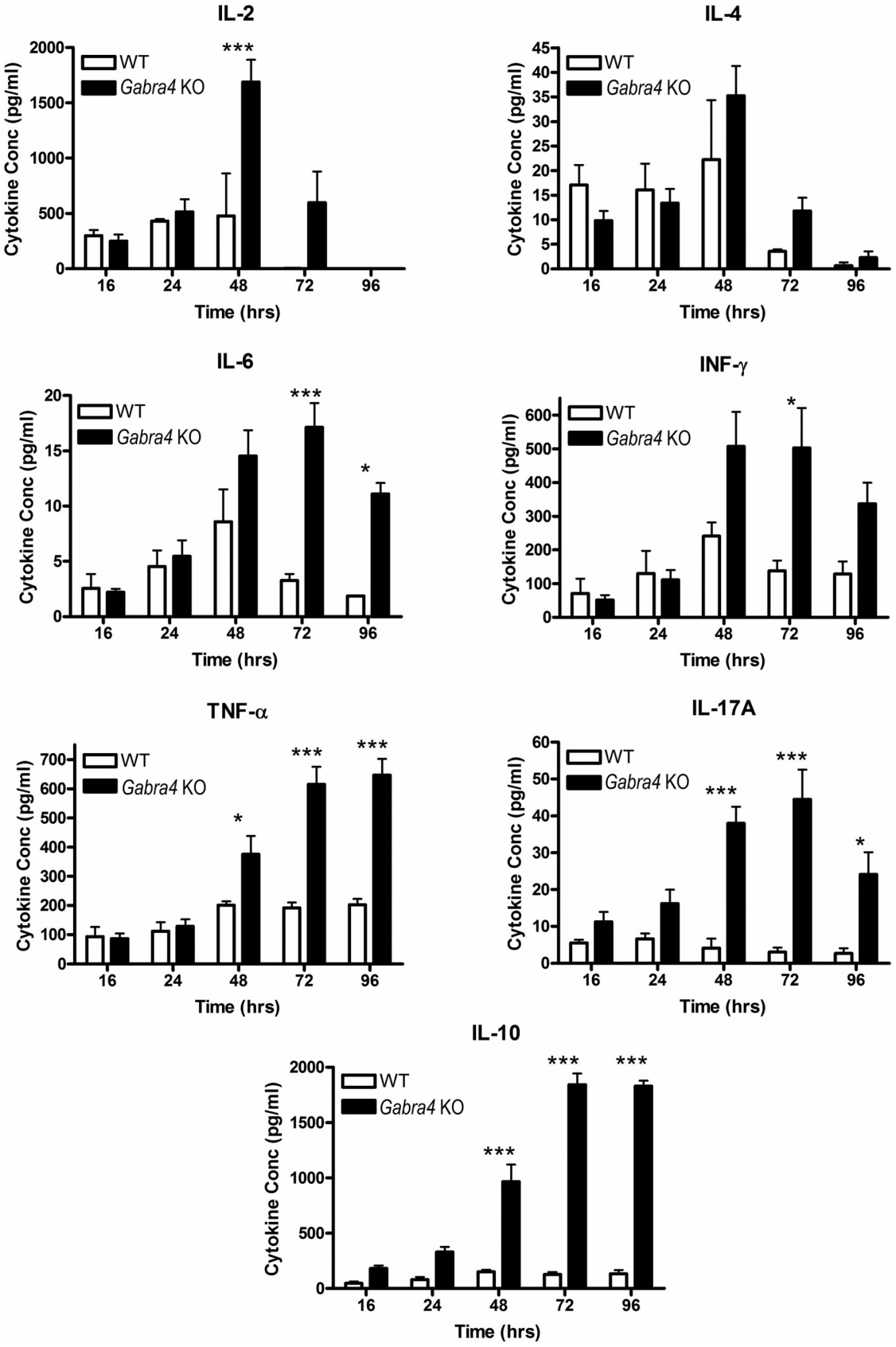

Fig. 6. In vitro CD4$^+$ cell cytokine production. Follow stimulation with anti-CD3/28 coated beads, *Gabra4* KO and WT CD4$^+$ lymphocyte cell culture supernatant concentrations of several cytokines were measure at multiple time points over 96 h. *Gabra4* KO CD4$^+$ cells produced significantly higher concentrations of multiple cytokines (pro- and anti-inflammatory) at multiple time points. ANOVA with Bonferroni post hoc comparisons. Data are means ± SE; $n = 3$ mice. *$P < 0.05$. ***$P < 0.001$.

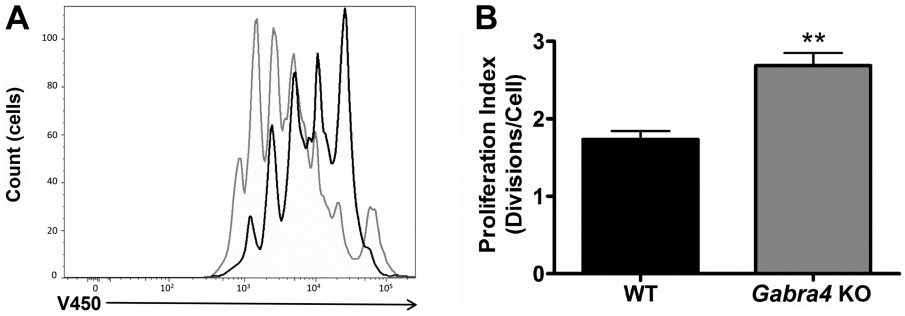

Fig. 7. In vitro $CD4^+$ cell proliferation. Following stimulation with anti-CD8/28 beads for 72 h, *Gabra4* KO and WT $CD4^+$ cell proliferation was assayed by fluorescein diacetate dilution. As demonstrated in the representative tracings (*A*; black tracing is WT, and gray tracing is *Gabra4* KO) and as quantified by proliferation index (*B*), *Gabra4* KO $CD4^+$ cells proliferated significantly more than WT cells. Data are means ± SE; $n = 3$ mice. $^{**}P > 0.01$ by Student's *t*-test.

Mechanistically, it is not yet clearly understood how genetic deletion of the $GABA_AR$ α_4-subunit leads to changes in the inflammatory response to HDM. Given the evidence that we and others have presented demonstrating α_4-subunit-containing $GABA_AR$ expression on immune cells (1, 3, 7, 25, 32, 36, 43), we hypothesize that the difference in the immune response to HDM is a result of alterations in peripheral immune cell function. Consistent with this, we demonstrated that *Gabra4* KO $CD4^+$ cells, key mediators of allergic inflammatory responses, are "hyperresponsive" to T-cell receptor stimulation in vitro. These cells express higher levels of several proinflammatory cytokines, with altered kinetics (i.e., prolonged activation), and proliferated more rapidly than WT $CD4^+$ cells under the same conditions. In vivo, such $CD4^+$ cells might behave similarly, orchestrating a heightened immune response to HDM, which ultimately results in heightened airway reactivity. This is consistent with our studies of intrapulmonary immune cells in the present study, as we demonstrate that $CD4^+$ cells in *Gabra4* KO mice express higher levels of activation/memory markers than WT mice after 3 wk of HDM-sensitization, despite a relative loss of total number of lymphocytes demonstrated on FSC/SSC analysis.

Because the $GABA_AR$ is an ion channel, one might assume that knockout of the α_4-subunit would only affect lymphocyte function if alterations in lymphocyte membrane potential affect key cellular processes. Lymphocytes are not considered "excitable" cells in the way neurons or muscle cells are, but they do express a number of ion channels and alterations in membrane potential can drastically affect lymphocyte activation in response to antigen (23). For example, inhibition of certain plasma membrane potassium channels, which results in a depolarization of membrane potential, significantly inhibits T-cell activation (6, 19, 20, 23, 35). In fact, there is significant interest in utilizing potassium channel inhibitors to treat a number of autoimmune diseases (2, 31), including multiple sclerosis (44) and alopecia areata (12). This membrane potential-dependent lymphocyte inhibition likely results in altered cellular calcium dynamics. Effective T-cell activation following antigen presentation to the T-cell receptor requires cytosolic calcium levels to be elevated for a period of ~1–2 h to induce and maintain nuclear factor of activated T cells in its transcriptionally active state within the nucleus (21). Initially, this calcium elevation results from phospholipase C/1,4,5-inositol trisphosphate-mediated endoplasmic reticulum (ER) calcium release. However, lymphocyte ER calcium stores are insufficient to produce the necessary elevation in calcium concentration required for T-cell activation. Calcium must enter from the extracellular space (21). In lymphocytes, the majority of this calcium enters via a process termed store-operated calcium entry, which has been well described (22). Briefly, following ER calcium release, low ER concentrations of calcium are detected by STIM1, which then forms a complex with Orai1 in the plasma membrane that serves as a channel for calcium entry. Although this complex is not voltage gated, calcium entry the STIM-Orai complex is subject to changes in its electrochemical driving force. This is thought to be the mechanism by which potassium channel inhibitors suppress antigen-driven lymphocyte activation (23). Opening a $GABA_AR$ is also predicted to depolarize lymphocyte membrane potentials by allowing chloride efflux [due to a resting membrane potential of approximately −50 to −70 and a high intracellular chloride concentration estimated to be 56 mM (30), although possibly even as high as 80 mM] (11). This may inhibit calcium entry and cellular activation in a fashion similar to inhibiting potassium channels.

Some $GABA_ARs$, particularly those located in CNS extrasynaptic sites and those located outside of the CNS, produce tonic chloride currents. These tonic currents may exist in lymphocytes providing a tonic depolarizing contribution to membrane potential. Global knockout of the $GABA_AR$ α_4-subunit may diminish this tonic current, causing the membrane potential to become relatively hyperpolarized. This would favor calcium influx via the STIM-Orai complex after antigen presentation to the T-cell receptor, leading to a state of heightened cellular activation and potentially apoptosis, another calcium-dependent process (27). This may explain the heightened inflammatory state of the $GABA_AR$ α_4-KO mice and the apparent apoptosis of their lymphocytes.

Alternatively, it is interesting to note that, in addition to chloride, $GABA_ARs$ are permeant to bicarbonate. Thus activation of $GABA_AR$ decreases intracellular pH (17, 18). Given the small size of a lymphocyte, this drop could be particularly significant. The pore region of Orai1 is highly basic (a glutamate serves as selectivity filter) (14), and calcium conductance through Orai1 is significantly hindered by decreases in intra- and extracellular pH (40). Thus $GABA_AR$ activation may inhibit store-operated calcium entry not by depolarizing membrane potential but by intracellular acidification. Further studies into these hypotheses are underway.

Given the important role that $GABA_ARs$ play in CNS inhibitory neurotransmission, it is also possible that the heightened immune response demonstrated here in *Gabra4* KO mice is a result of alterations in CNS signaling. In recent years, several elegant studies have demonstrated that CNS outputs have significant effects on the immune system, including the so-called "inflammatory reflex" by which vagal nerve signaling

into the spleen serves as a check on systemic inflammation (29, 39). It is possible that the change in $GABA_AR$ signaling that results from *Gabra4* KO leads to an alteration in CNS outputs that modulate the immune response. It should be noted that these mice appear neurologically normal and differences in neurologic assessment have only been demonstrated in the mice's response to a certain neurosteroid (15). Furthermore, the in vitro $CD4^+$ cell cytokine and production data presented here argue that a peripheral immune cell-mediated effect is contributing to the increased inflammatory state seen in *Gabra4* KO mice. However, these considerations do not rule out the possible contribution of CNS-mediated mechanisms.

Although a model of inflammatory asthma is presented here, there is no reason to believe that $GABA_AR$ signaling might not also modulate immune function in other physiologic and pathophysiologic processes. These include infectious states like sepsis, inflammatory responses like systemic immune response syndrome and acute respiratory distress syndrome, and chronic autoimmune diseases. In fact, tumor surveillance might also be affected by $GABA_AR$ signaling, providing a potential mechanistic link between anesthetic exposure and cancer recurrence. Given the widespread use of $GABA_AR$-modulating drugs in clinical anesthesia practice, both in operating rooms and in intensive care units, more research is warranted to understand their potential implications on immune function.

In summary, this study demonstrates that murine lymphocytes express mRNA encoding multiple $GABA_AR$ subunits, including that of the α_4-subunit, and that global knockout of the $GABA_AR$ α_4-subunit leads to a more severe asthmatic phenotype in a murine inflammatory/allergic asthma model, both in terms of in vivo airway reactivity and airway inflammation. This increased reactivity is likely the result of the increased inflammation, not a direct smooth muscle effect, as ex vivo organ bath experiments showed no difference in the contractile properties of WT and $GABA_AR$ α_4-subunit KO tracheal rings. We propose that, under normal conditions, chloride and/or bicarbonate currents mediated by $GABA_AR$ channels act to restrict immune cell activation by limiting calcium entry through the STIM-Orai complex. Furthermore, this effect may be diminished in *Gabra4* KO mice, making their immune cells more "excitable." Further mechanistic studies are required to understand $GABA_AR$ signaling events in immune cells.

ACKNOWLEDGMENTS

Present address of D. L. Turner: Dept. of Biology, Williams College, Williamstown, MA.

GRANTS

This work was supported by the Foundation for Anesthesia Education and Research (G. T. Yocum and J. Danielsson), the Stony Wold-Herbert Fund (to G. T. Yocum and J. Danielsson), and National Institutes of Health Grants GM-065281 (to C. W. Emala and G. T. Yocum), AA-10422 (to G. E. Homanic), and HL-122340 (to C. W. Emala). A portion of the research reported in this publication was performed in the Columbia Center for Translational Immunology Flow Cytometry Core, supported in part by the Office of the Director, National Institutes of Health Award S10-RR-027050.

DISCLOSURES

No conflicts of interest, financial or otherwise, are declared by the authors.

AUTHOR CONTRIBUTIONS

G.T.Y., D.L.T., J.D., M.B.B., Y.Z., D.X., N.H., G.E.H., D.L.F., and C.W.E. conceived and designed research; G.T.Y., D.L.T., J.D., M.B.B., Y.Z., and D.X. performed experiments; G.T.Y., D.L.T., J.D., M.B.B., Y.Z., D.X., D.L.F., and C.W.E. analyzed data; G.T.Y., D.L.T., J.D., M.B.B., D.X., N.H., G.E.H., D.L.F., and C.W.E. interpreted results of experiments; G.T.Y. and D.L.T. prepared figures; G.T.Y. drafted manuscript; G.T.Y., D.L.T., J.D., M.B.B., Y.Z., D.X., N.H., G.E.H., D.L.F., and C.W.E. edited and revised manuscript; G.T.Y., D.L.T., J.D., M.B.B., Y.Z., D.X., N.H., G.E.H., D.L.F., and C.W.E. approved final version of manuscript.

REFERENCES

1. **Alam S, Laughton DL, Walding A, Wolstenholme AJ.** Human peripheral blood mononuclear cells express $GABA_A$ receptor subunits. *Mol Immunol* 43: 1432–1442, 2006. doi:10.1016/j.molimm.2005.07.025.
2. **Beeton C, Wulff H, Standifer NE, Azam P, Mullen KM, Pennington MW, Kolski-Andreaco A, Wei E, Grino A, Counts DR, Wang PH, LeeHealey CJ, S Andrews B, Sankaranarayanan A, Homerick D, Roeck WW, Tehranzadeh J, Stanhope KL, Zimin P, Havel PJ, Griffey S, Knaus HG, Nepom GT, Gutman GA, Calabresi PA, Chandy KG.** Kv1.3 channels are a therapeutic target for T cell-mediated autoimmune diseases. *Proc Natl Acad Sci USA* 103: 17414–17419, 2006. doi:10.1073/pnas.0605136103.
3. **Bhat R, Axtell R, Mitra A, Miranda M, Lock C, Tsien RW, Steinman L.** Inhibitory role for GABA in autoimmune inflammation. *Proc Natl Acad Sci USA* 107: 2580–2585, 2010. doi:10.1073/pnas.0915139107.
4. **Bousquet J, Chanez P, Lacoste JY, Barnéon G, Ghavanian N, Enander I, Venge P, Ahlstedt S, Simony-Lafontaine J, Godard P, Michel FB.** Eosinophilic inflammation in asthma. *N Engl J Med* 323: 1033–1039, 1990. doi:10.1056/NEJM199010113231505.
5. **Chandra D, Jia F, Liang J, Peng Z, Suryanarayanan A, Werner DF, Spigelman I, Houser CR, Olsen RW, Harrison NL, Homanics GE.** $GABA_A$ receptor alpha 4 subunits mediate extrasynaptic inhibition in thalamus and dentate gyrus and the action of gaboxadol. *Proc Natl Acad Sci USA* 103: 15230–15235, 2006. doi:10.1073/pnas.0604304103.
6. **Chandy KG, DeCoursey TE, Cahalan MD, McLaughlin C, Gupta S.** Voltage-gated potassium channels are required for human T lymphocyte activation. *J Exp Med* 160: 369–385, 1984. doi:10.1084/jem.160.2.369.
7. **Dionisio L, José De Rosa M, Bouzat C, Esandi MC.** An intrinsic GABAergic system in human lymphocytes. *Neuropharmacology* 60: 513–519, 2011. doi:10.1016/j.neuropharm.2010.11.007.
8. **Gallos G, Gleason NR, Zhang Y, Pak SW, Sonett JR, Yang J, Emala CW.** Activation of endogenous $GABA_A$ channels on airway smooth muscle potentiates isoproterenol-mediated relaxation. *Am J Physiol Lung Cell Mol Physiol* 295: L1040–L1047, 2008. doi:10.1152/ajplung.90330.2008.
9. **Gallos G, Yim P, Chang S, Zhang Y, Xu D, Cook JM, Gerthoffer WT, Emala CW Sr.** Targeting the restricted α-subunit repertoire of airway smooth muscle $GABA_A$ receptors augments airway smooth muscle relaxation. *Am J Physiol Lung Cell Mol Physiol* 302: L248–L256, 2012. doi:10.1152/ajplung.00131.2011.
10. **Gallos G, Yocum GT, Siviski ME, Yim PD, Fu XW, Poe MM, Cook JM, Harrison N, Perez-Zoghbi J, Emala CW Sr.** Selective targeting of the α_5-subunit of $GABA_A$ receptors relaxes airway smooth muscle and inhibits cellular calcium handling. *Am J Physiol Lung Cell Mol Physiol* 308: L931–L942, 2015. doi:10.1152/ajplung.00107.2014.
11. **Garcia-Soto JJ, Grinstein S.** Determinants of the transmembrane distribution of chloride in rat lymphocytes: role of Cl^--HCO_3^- exchange. *Am J PhysiolCell Physiol* 258: C1108–C1116, 1990.
12. **Gilhar A, Keren A, Shemer A, Ullmann Y, Paus R.** Blocking potassium channels (Kv1.3): a new treatment option for alopecia areata? *J Invest Dermatol* 133: 2088–2091, 2013. doi:10.1038/jid.2013.141.
13. **Haenisch B, Huber M, Wilhelm T, Steffens M, Molderings GJ.** Investigation into mechanisms mediating the inhibitory effect of 1,4-benzodiazepines on mast cells by gene expression profiling. *Life Sci* 92: 345–351, 2013. doi:10.1016/j.lfs.2013.01.010.
14. **Hou X, Pedi L, Diver MM, Long SB.** Crystal structure of the calcium release-activated calcium channel Orai. *Science* 338: 1308–1313, 2012. doi:10.1126/science.1228757.
15. **Iyer SV, Chandra D, Homanics GE.** GABAA-R α4 subunits are required for the low dose locomotor stimulatory effect of alphaxalone, but not for several other behavioral responses to alphaxalone, etomidate or propofol. *Neurochem Res* 39: 1048–1056, 2014. doi:10.1007/s11064-013-1148-3.

16. **Jin HS, Park Y, Elly C, Liu YC.** Itch expression by Treg cells controls Th2 inflammatory responses. *J Clin Invest* 123: 4923–4934, 2013. doi:10.1172/JCI69355.
17. **Kaila K, Saarikoski J, Voipio J.** Mechanism of action of GABA on intracellular pH and on surface pH in crayfish muscle fibres. *J Physiol* 427: 241–260, 1990. doi:10.1113/jphysiol.1990.sp018170.
18. **Kaila K, Voipio J.** Postsynaptic fall in intracellular pH induced by GABA-activated bicarbonate conductance. *Nature* 330: 163–165, 1987. doi:10.1038/330163a0.
19. **Koo GC, Blake JT, Talento A, Nguyen M, Lin S, Sirotina A, Shah K, Mulvany K, Hora D Jr, Cunningham P, Wunderler DL, McManus OB, Slaughter R, Bugianesi R, Felix J, Garcia M, Williamson J, Kaczorowski G, Sigal NH, Springer MS, Feeney W.** Blockade of the voltage-gated potassium channel Kv1.3 inhibits immune responses in vivo. *J Immunol* 158: 5120–5128, 1997.
20. **Leonard RJ, Garcia ML, Slaughter RS, Reuben JP.** Selective blockers of voltage-gated K^+ channels depolarize human T lymphocytes: mechanism of the antiproliferative effect of charybdotoxin. *Proc Natl Acad Sci USA* 89: 10094–10098, 1992. doi:10.1073/pnas.89.21.10094.
21. **Lewis RS.** Calcium signaling mechanisms in T lymphocytes. *Annu Rev Immunol* 19: 497–521, 2001. doi:10.1146/annurev.immunol.19.1.497.
22. **Lewis RS.** Store-operated calcium channels: new perspectives on mechanism and function. *Cold Spring Harb Perspect Biol* 3: a003970, 2011. doi:10.1101/cshperspect.a003970.
23. **Lewis RS, Cahalan MD.** Potassium and calcium channels in lymphocytes. *Annu Rev Immunol* 13: 623–653, 1995. doi:10.1146/annurev.iy.13.040195.003203.
24. **Masoli M, Fabian D, Holt S, Beasley R; Global Initiative for Asthma (GINA) Program.** The global burden of asthma: executive summary of the GINA Dissemination Committee report. *Allergy* 59: 469–478, 2004. doi:10.1111/j.1398-9995.2004.00526.x.
25. **Mendu SK, Bhandage A, Jin Z, Birnir B.** Different subtypes of GABA-A receptors are expressed in human, mouse and rat T lymphocytes. *PLoS One* 7: e42959, 2012. doi:10.1371/journal.pone.0042959.
26. **Mizuta K, Xu D, Pan Y, Comas G, Sonett JR, Zhang Y, Panettieri RA Jr, Yang J, Emala CW Sr.** $GABA_A$ receptors are expressed and facilitate relaxation in airway smooth muscle. *Am J Physiol Lung Cell Mol Physiol* 294: L1206–L1216, 2008. doi:10.1152/ajplung.00287.2007.
27. **Orrenius S, Zhivotovsky B, Nicotera P.** Regulation of cell death: the calcium-apoptosis link. *Nat Rev Mol Cell Biol* 4: 552–565, 2003. doi:10.1038/nrm1150.
28. **Pandharipande PP, Sanders RD, Girard TD, McGrane S, Thompson JL, Shintani AK, Herr DL, Maze M, Ely EW; MENDS Investigators.** Effect of dexmedetomidine versus lorazepam on outcome in patients with sepsis: an a priori-designed analysis of the MENDS randomized controlled trial. *Crit Care* 14: R38, 2010. doi:10.1186/cc8916.
29. **Pavlov VA, Tracey KJ.** Neural circuitry and immunity. *Immunol Res* 63: 38–57, 2015. doi:10.1007/s12026-015-8718-1.
30. **Pilas B, Durack G.** A flow cytometric method for measurement of intracellular chloride concentration in lymphocytes using the halide-specific probe 6-methoxy-N-(3-sulfopropyl) quinolinium (SPQ). *Cytometry* 28: 316–322, 1997. doi:10.1002/(SICI)1097-0320(19970801)28:4<316::AID-CYTO7>3.0.CO;2-9.
31. **Rashid MH, Huq R, Tanner MR, Chhabra S, Khoo KK, Estrada R, Dhawan V, Chauhan S, Pennington MW, Beeton C, Kuyucak S, Norton RS.** A potent and Kv1.3-selective analogue of the scorpion toxin HsTX1 as a potential therapeutic for autoimmune diseases. *Sci Rep* 4: 4509, 2014. doi:10.1038/srep04509.
32. **Reyes-García MG, Hernández-Hernández F, Hernández-Téllez B, García-Tamayo F.** GABA (A) receptor subunits RNA expression in mice peritoneal macrophages modulate their IL-6/IL-12 production. *J Neuroimmunol* 188: 64–68, 2007. doi:10.1016/j.jneuroim.2007.05.013.
33. **Riker RR, Shehabi Y, Bokesch PM, Ceraso D, Wisemandle W, Koura F, Whitten P, Margolis BD, Byrne DW, Ely EW, Rocha MG, Group SS; SEDCOM (Safety and Efficacy of Dexmedetomidine Compared With Midazolam) Study Group.** Dexmedetomidine vs midazolam for sedation of critically ill patients: a randomized trial. *JAMA* 301: 489–499, 2009. doi:10.1001/jama.2009.56.
34. **Sanders RD, Godlee A, Fujimori T, Goulding J, Xin G, Salek-Ardakani S, Snelgrove RJ, Ma D, Maze M, Hussell T.** Benzodiazepine augmented γ-amino-butyric acid signaling increases mortality from pneumonia in mice. *Crit Care Med* 41: 1627–1636, 2013. doi:10.1097/CCM.0b013e31827c0c8d.
35. **Schlichter L, Sidell N, Hagiwara S.** Potassium channels mediate killing by human natural killer cells. *Proc Natl Acad Sci USA* 83: 451–455, 1986. doi:10.1073/pnas.83.2.451.
36. **Tian J, Chau C, Hales TG, Kaufman DL.** GABA(A) receptors mediate inhibition of T cell responses. *J Neuroimmunol* 96: 21–28, 1999. doi:10.1016/S0165-5728(98)00264-1.
37. **Townsend EA, Emala CW Sr.** Quercetin acutely relaxes airway smooth muscle and potentiates β-agonist-induced relaxation via dual phosphodiesterase inhibition of PLCβ and PDE4. *Am J Physiol Lung Cell Mol Physiol* 305: L396–L403, 2013. doi:10.1152/ajplung.00125.2013.
38. **Townsend EA, Siviski ME, Zhang Y, Xu C, Hoonjan B, Emala CW.** Effects of ginger and its constituents on airway smooth muscle relaxation and calcium regulation. *Am J Respir Cell Mol Biol* 48: 157–163, 2013. doi:10.1165/rcmb.2012-0231OC.
39. **Tracey KJ.** The inflammatory reflex. *Nature* 420: 853–859, 2002. doi:10.1038/nature01321.
40. **Tsujikawa H, Yu AS, Xie J, Yue Z, Yang W, He Y, Yue L.** Identification of key amino acid residues responsible for internal and external pH sensitivity of Orai1/STIM1 channels. *Sci Rep* 5: 16747, 2015. doi:10.1038/srep16747.
41. **Uhm TG, Kim BS, Chung IY.** Eosinophil development, regulation of eosinophil-specific genes, and role of eosinophils in the pathogenesis of asthma. *Allergy Asthma Immunol Res* 4: 68–79, 2012. doi:10.4168/aair.2012.4.2.68.
42. **Wang JY.** The innate immune response in house dust mite-induced allergic inflammation. *Allergy Asthma Immunol Res* 5: 68–74, 2013. doi:10.4168/aair.2013.5.2.68.
43. **Wheeler DW, Thompson AJ, Corletto F, Reckless J, Loke JC, Lapaque N, Grant AJ, Mastroeni P, Grainger DJ, Padgett CL, O'Brien JA, Miller NG, Trowsdale J, Lummis SC, Menon DK, Beech JS.** Anaesthetic impairment of immune function is mediated via GABA(A) receptors. *PLoS One* 6: e17152, 2011. doi:10.1371/journal.pone.0017152.
44. **Wulff H, Calabresi PA, Allie R, Yun S, Pennington M, Beeton C, Chandy KG.** The voltage-gated Kv1.3 $K(^+)$ channel in effector memory T cells as new target for MS. *J Clin Invest* 111: 1703–1713, 2003. doi:10.1172/JCI16921.
45. **Yocum GT, Gallos G, Zhang Y, Jahan R, Stephen MR, Varagic Z, Puthenkalam R, Ernst M, Cook JM, Emala CW.** Targeting the gamma-aminobutyric acid A receptor alpha4 subunit in airway smooth muscle to alleviate bronchoconstriction. *Am J Respir Cell Mol Biol* 54: 546–553, 2016. doi:10.1165/rcmb.2015-0176OC.